Proceedings of the Korean Nuclear Society Spring Meeting
Cheju, Korea, May 1996

A Modification of Departure from Nucleate Boiling Model Based on Mass, Energy, and Momentum Balance For Subcooled Flow Boiling in Vertical Tubes

Young Sil Sul, Kwang Won Lee, Kyong In Ju, Jong Sik Cheong, and Jae Young Yang
Korea Atomic Energy Research Institute

Abstract

Several analytical models for the departure from nucleate boiling (DNB) phenomenon have been developed during the last decade. Among these, Chang & Lee's model based on a bubble crowding mechanism is remarkable in the fundamental features characterized as the formulation of mass, energy, and momentum balance equations at thermal-hydraulic conditions leading to the DNB. However, Bricard and Souyri remarked that the assumption of stagnant bubbly layer at the DNB condition is questionable and the signs on the axial projections of the momentum fluxes at the core/bubbly layer interface in the momentum balance equations are erroneous. From this remark, Chang & Lee's model has been re-examined and modified by correcting the erroneous treatments in the momentum balance equations and removing the spurious assumptions. The revised model predicts well the extensive DNB data of water in uniformly heated tubes at low qualities and shows more accurate prediction compared with the original model.

1. Introduction

Analytical departure from nucleate boiling (DNB) models for the low quality flow boiling can be devided into two categories based on the DNB mechanism, namely, bubble crowding models and liquid sublayer dryout models. Weisman and co-workers[1,2] and Chang & Lee[3] have developed the bubble crowding models. Chang & Lee[3] formulated fundamentally the DNB formula based on the mass, energy, and momentum balance equations with the bubble crowding concept as the crucial DNB mechanism, while Weisman and co-workers formulated the DNB formula based on a semi-empirical two-phase mixture turbulence model. To derive the DNB formula from the balance equations, Chang & Lee supposed the assumption of stagnant bubbly layer at the DNB condition. However, Bricard and Souyri[4] remarked that some basic relations of the Chang & Lee model are erroneous (the axial projections of the momentum fluxes at the core/bubbly layer interface are written with the wrong sign in the momentum balance equations) or questionable (since the bubbly layer is assumed stagnant, the axial projections of the momentum fluxes at the core/bubbly layer interface should be null). From this remark, Chang & Lee's model has been re-examined and it is found that the stagnancy of the bubbly layer and the zero wall shear stress resulting from this stagnancy are wrong and spurious assumptions. Originally, these assumptions were used to eliminate the wall shear stress(τ_{wb}) and the bubbly layer velocity (U_b) terms in the balance equations. But, these assumptions resulted in an inconsistency and erroneous conclusion in the momentum balance equations.

The purpose of this work is to correct the erroneous treatments in the momentum balance equations, to remove the spurious assumptions, and to develop a more generalized and mechanistic DNB model involving the effects of bubbly layer flow structure and void fraction on the wall and interfacial shear stresses. The predictions of the modified model are compared with the extensive DNB data of water in uniformly heated tubes at low qualities in order to show the validity of the modified model and also compared with those of the original model in order to show the enhancement of the modified model.

2. Model Development

2.1 Model Description

The physical model proposed for transport phenomena in the vicinity of the DNB location is based on the concept of bubble crowding as the DNB mechanism and is illustrated schematically in Figure 1. To derive the DNB formula from the balance equations, Chang & Lee supposed the following four postulates for the DNB condition as the limiting conditions of the thermal transport on the bubbly layer:

(1) Due to bubble crowding near the wall, a stagnant bubbly layer with rigid packing ellipsoidal bubbles can occur at the thin layer adjacent to the wall. The ellipsoidal shape of bubbles seems to be due to bubble flattening effect by highly heated wall. This bubbly layer is maintained until a thermal transport limitation condition is reached.
(2) At this situation the wall shear stress of the bubbly layer becomes zero. The friction force of bulk flow is only concentrated on the bubbly-core interface.
(3) DNB condition reaches when a radial thermal transport rates is limited by equal flows to and away from the interface.
(4) The thermal transport limitation is quantified by local mass, energy, and momentum balance equations rather than a BLS condition or the characteristics of two-phase mixture turbulence.

From the above postulates and the analogy between evaporative momentum flux term in the momentum balance equations of separated flow model[5] and net interfacial momentum term at the core/bubbly layer interface, the following momentum equations were derived.

$$-\frac{dP}{dz} - \rho_b g - \frac{\tau_{wb}\,\hat{\xi}_w}{A(1-\langle\alpha_c\rangle)} + \frac{\tau_{wi}\,\hat{\xi}_i}{A(1-\langle\alpha_c\rangle)} - \frac{(G_{cb}\langle U_c\rangle_c - G_{bc}\langle U_b\rangle_b)\,\hat{\xi}_i}{A(1-\langle\alpha_c\rangle)} = \rho_b\langle U_b\rangle_b\frac{d\langle U_b\rangle_b}{dz} \quad \text{for the bubbly layer} \tag{1}$$

$$-\frac{dP}{dz} - \rho_c g - \frac{\tau_{wi}\,\hat{\xi}_i}{A\langle\alpha_c\rangle} + \frac{(G_{cb}\langle U_c\rangle_c - G_{bc}\langle U_b\rangle_b)\,\hat{\xi}_i}{A\langle\alpha_c\rangle} = \rho_c\langle U_c\rangle_c\frac{d\langle U_c\rangle_c}{dz} \quad \text{for the core region} \tag{2}$$

As the DNB condition, Chang & Lee supposed that the mass transport rate at the core/bubbly layer interface is limited and thus

$$G_{cb} = G_{bc} = G^* \tag{3}$$

After subtracting Eq.(1) from Eq.(2) to eliminating the pressure gradient term, we obtain the following relative motion equation at the DNB condition:

$$-(\rho_c-\rho_b)g + \frac{\tau_{wb}\,\hat{\xi}_w}{A(1-\langle\alpha_c\rangle)} - \frac{\tau_{wi}\,\hat{\xi}_i}{A\langle\alpha_c\rangle(1-\langle\alpha_c\rangle)} + \frac{G^*\overline{U_r}}{A\langle\alpha_c\rangle(1-\langle\alpha_c\rangle)} = \rho_c\langle U_c\rangle_c\frac{d\langle U_c\rangle_c}{dz} - \rho_b\langle U_b\rangle_b\frac{d\langle U_b\rangle_b}{dz} \tag{4}$$

While deriving the above momentum balance equations, Chang & Lee considered an evaporative momentum flux as a net interfacial momentum (i.e., $G_{cb}\langle U_c\rangle_c - G_{bc}\langle U_b\rangle_b$) to obtain a positive value of the limited mixing mass flux (G^*) at the DNB condition in Eq.(4). However, the Eqs.(1) and (2) have the wrong sign in the axial projections of the momentum fluxes at the core/bubbly layer interface as Bricard and Souyri pointed out in Reference 4. After correcting the wrong sign in the above momentum equations (the signs of the fifth term of LHS of Eq.(1) and the fourth term of LHS of Eq.(2) are reversed), G^* resulted in negative at the supposed DNB condition. Since physically G^* must be positive, it seems that something happens to be wrong in postulates for the DNB condition. From the re-examination of the basic postulates and skin friction factor model, it is found that the

stagnancy of the bubbly layer in the first postulate and the zero wall shear stress resulting from this stagnancy in the second postulate are wrong and spurious assumptions. Due to the misunderstanding upon the interfacial momentum exchange and the wall shear stress in the roughened wall with rigid bubbles, these spurious assumptions seem to be introduced.

After discarding these assumptions, correcting the wrong sign and using some two-phase flow identities defined in Reference 3, we can obtain the following new equation for the limited mixing mass flux, G^* :

$$G^{*2}=\left\{-(\rho_c-\rho_b)g+\frac{\tau_{wb}\langle\alpha_c\rangle\hat{\xi}_w-\tau_{wi}\hat{\xi}_i}{A\langle\alpha_c\rangle(1-\langle\alpha_c\rangle)}+\left[\frac{G\langle x_c\rangle}{\rho_c\langle\alpha_c\rangle}\right]^2\frac{d\rho_c}{dz}\right\}\frac{A\langle\alpha_c\rangle(1-\langle\alpha_c\rangle)}{\overline{U_r}\hat{\xi}_i} \quad (5)$$

Other equations in Reference 3 are not affected by the removal of these assumptions if the following assumption and approximations are used:

(1) the critical density and quality of bubbly layer at the DNB condition remain constant ($d\rho_b/dz=0$; $d\chi_{gb}/dz=0$).

(2) the mass flux and average velocity of bubbly layer are negligible compared with those of core region ($U_c-U_b\approx U_c$).

2.2 Constitutive Equations

To quantify the shear stress term in Eq.(5), the skin friction factor model is required. Through the review of the multi-parameter roughness model of Beattie[6], it is found that the Nedderman-Shearer friction factor equation chosen by Chang & Lee was based on the multi-parameter roughness model instead of a single parameter roughness model. The former is able to consider the effective viscosity in the near wall region as well as the influence of roughness element shape & density and the origin of the turbulent core logarithmic layer upon the evaluation of the roughness effect on classical turbulence theory, while the latter is based on only roughness height, i.e., equivalent sand roughness. In fact, the Nedderman-Shearer equation can have the physical basis only in the cases that the roughness size is uniform and the origin of the turbulence core equals to $y^+=12$. If the bubbly layer thickness is considered as the equivalent sand roughness height, ε, the shear stress determined by the Nedderman-Shearer equation should be considered as an approximate wall shear stress acting on the top of roughness element, i.e., the core/bubbly layer interface. Here, the bubbly layer is assumed to be located considerably below the turbulent core origin. Originally, this stress was considered as the interfacial shear stress having upward force direction, since this stress acts on not the wall surface but the interface. However, this stress should be considered as the approximate wall shear stress upon the interface having downward force direction, since the Nedderman-Shearer equation was derived by averaging the turbulent core logarithmic velocity profile having the origin of $y^+=12$ over the flow cross section. Therefore, the second term in the RHS of Eq.(5) can be approximated at the DNB condition as follows:

$$\frac{\tau_{wb}\langle\alpha_c\rangle\hat{\xi}_w-\tau_{wi}\hat{\xi}_i}{A\langle\alpha_c\rangle(1-\langle\alpha_c\rangle)}\approx\frac{\tau_{wb}\hat{\xi}_i}{A\langle\alpha_c\rangle(1-\langle\alpha_c\rangle)} \quad (6)$$

This approximation shows that at the DNB condition the interfacial shear stress disappears and the wall shear stress having downward force direction at the core/bubbly interface becomes domonant, since the bubbly layer is considered as the roughness element within the viscous sublayer boundary ($y^+=12$). For this reason, the interfacial shear stress or skin friction factor in Eqs. (22), (24), (26), and (37) to (41) of the Reference 3 should be replaced by the wall shear stress or its friction factor.

In addition, the well-known void fraction and quality relationship based on the drift flux models of Chexal et al. [7] is used to find the void fraction (or quality) when the quality (or void fraction) is given. Furthermore, the flow regime map is used to identify the DNB mechanism and to validate our physical model. The flow regime map is based on Mishima and Ishii's flow transition criteria [8].

2.3 Resulting DNB formula

Finally, the resulting DNB equation, namely Eq.(42) of Reference 3, can be modified as follows:

$$q''_{DNB} = \frac{[-(\rho_c-\rho_b)gA\langle\alpha_c\rangle(1-\langle\alpha_c\rangle)/\xi_i+\tau_{wb}]\Delta x_g\xi_i\, h_{fg}\,\rho_c\langle\alpha_c\rangle}{G\xi_w\left\{F_q\langle x_c\rangle-(1-\langle\alpha_c\rangle)h_{fg}\frac{\Delta x_g}{\rho_c}\langle x_c\rangle^2\left[\frac{F_{AA}F_h}{(1-x_g)}+\frac{F_{AB}F_v}{h_{fg}\langle x_c\rangle}\right]\right\}} \quad (7)$$

The first term in the square bracket of numerator and the second term in the outer bracket of denominator are the buoyancy and acceleration terms, respectively. When compared with the original DNB formula, the buoyancy and acceleration terms have the opposite sign according to Eq.(5) and the fraction of mass flux in core region, $\langle x_c\rangle$ is considered in the acceleration term in order to quantify the reduction of $\langle x_c\rangle$ from the unity by the bubbly layer.

3. Results and Discussion

The predictions of the present model were compared with more than 700 DNB data points chosen from the data sources of References 9 to 12 by using the Mishima and Ishii's flow pattern map as a data selection tool. The chosen data points belong to the DNB data at the bubbly flow, slug flow and churn flow. The range of selected data is 6-20 MPa for pressure, 600-8000 kg/m^{2}s for mass flux and 20-700 for L/D.

To assess the dependence of the DNB formula on the acceleration term and the various constitutive models, seven simulations are performed. The features for each simulation are listed in Table 1. By introducing the relative accuracy defined as the ratio of predicted DNB to measured DNB, the results for each simulation are quantitatively compared with that of AECL Lookup table[13] and listed in Table 2. The modified model predicts more accurate and larger number of the selected DNB data compared with the original one. To show the visual comparison of the predicted and measured DNB and the dependences of the prediction accuracy on important parameters, Figures 2 through 6 are presented for the simulation results of RUN1. Figure 2 shows that the predictions agree with the extensive DNB data within $\pm$20% error bounds. Some points in the outside of error bounds belong to the predictions at the small ratios of length to diameter (L/D$\leq$60). These overestimations seem to be due to a flow instability in the short tubes, which is not considered in the modified model.

4. Conclusion

The modification of Chang & Lee's model has been performed and results are summarized as follows:

(1) The sign changes in the buoyancy and acceleration terms have a little influence on the DNB prediction capability, since the effects of these terms in the domain of our interest are relatively small.

(2) The comparison of the predictions with the extensive DNB data of water shows that the DNB data can be predicted within $\pm$20 % error bounds by choosing two empirical constants adequately. The overall model accuracy (mean=1.09 and standard deviation=0.09) is comparable to that of AECL Lookup table (mean=1.01 and SD=0.088).

(3) Through several simulations it is found that the influences of the acceleration terms on the present DNB formula are negligible and that the fraction of mass flux in core, $\langle x_c\rangle$ has the considerable influence on the DNB formula.

References

[1] J. Weisman and B.S Pei, Prediction of CHF in flow boiling at low qualites, Int. J. Heat Mass Transfer 26 (1983) 1463.

[2] S.H Ying and J. Weisman, Prediction of CHF in flow boiling at intermediate qualites, Int. J. Heat Mass Transfer 29, No. 11 (1986) 1639-1648.

[3] Chang, S.H. & Lee, K.W., A critical heat flux model based on mass energy, and momentum

balance for upflow boiling at low qualities, Nuclear Engineering and Design, Vol. 113, 35-50, 1989.
[4] P. Bricard & A. Souyri, Understanding and modelling DNB in forced convective boiling : a critical review, International Symposium on Two Phase Flow Modelling & Experiments 1995, Rome, Italy, Vol.2, 843-851, October 9-11, 1995.
[5] R.T. Lahey Jr. and F. Moody, The thermal hydraulics of a boiling water nuclear reactor, Chapter 5, ANS, 1977.
[6] Beattie, A Smooth Tube Analogue of Roughened Wall Thermohydraulics, AERE-R 10194, 1981.
[7] B. Chexal, et al., A void fraction correlation for generalized applications, Proc. 4th Int. Topical Mtg, Nuclear Reactor Thermalhydrulics (NURETH), Karlsruhe, pp. 996-1002, 1989.
[8] K. Mishima and M. Ishii, Flow regime transition criteria for upward two-phase flow in vertical tubes, Int. J. Heat Mass Transfer, 27, pp. 723-737, 1984.
[9] B. Thompson and R. V. Macbeth, " Boiling Water Heat Transfer in Uniformly Heated Tubes : A Compilation of World Data with Accurate Correlations," AEEW-R-356, 1964.
[10] K. M. Becker et al., " Round Tube Burnout Data for Flow Boiling of Water at Pressures between 30 and 200 Bar," Report KTH-NEL-14, 1971.
[11] B. A. Zenkevich et al., " An Analysis and Correlation of the Experimental Data on Burnout in the Case of Forced Flow of Boiling Water in Pipes," Physico-Energy Institute, Atomizdat, Moscow, HTFS Translation 12022, 1969.
[12] W.H. Lowdermilk, C.D. Lanzo, and B.L. Siegel, Investigation of boiling burnout and flow stability for water flowing in tubes, NACA TN 4382, 1958.
[13] D.C. Groeneveld, et al., 1986 AECL-UO Critical heat flux lookup table, Heat Transfer Engineering, Vol. 7, 181-274, 1986.

Table 1 Features of Each Simulation Case

Simulation Number	Detached Bubble Diameter	Subcooled Model	Friction Factor Model	Acceleration Term	Selected Constant
RUN 1	Modified Levy	Saha & Zuber	Nedderman-Shearer	yes	α_{gt} =0.75, k=1.5
RUN 2	Modified Levy	Saha & Zuber	Nedderman-Shearer	no	α_{gt} =0.75, k=1.5
RUN 3	Rogers et al.	Rogers et al.	Nedderman-Shearer	yes	α_{gt} =0.75, k=1.5
RUN 4	Staub	Staub	Nedderman-Shearer	yes	α_{gt} =0.75, k=1.5
RUN 5	Modified Levy	Saha & Zuber	Colebrook-White	yes	α_{gt} =0.75, k=1.5
RUN 6	Modified Levy	Saha & Zuber	Nedderman-Shearer	yes	α_{gt} =0.70, k=2.0
RUN 7	Modified Levy	Saha & Zuber	Nedderman-Shearer	yes	α_{gt} =0.60, k=3.0

Table 2 Comparison of Predictability of Each Simulation with That of AECL Lookup Table[#]

Simulation Number	Mean Accuracy Ratio	Standard Deviation	Number of Predictions[##]
RUN 1	1.093 (1.092)	0.090 (0.095)	726 (629)
RUN 2	1.103 (1.076)	0.092 (0.097)	726 (628)
RUN 3	1.088 (0.981)	0.130 (0.148)	730 (537)
RUN 4	1.213 (0.981)	0.166 (0.148)	732 (537)
RUN 5	1.111 (1.102)	0.098 (0.097)	727 (629)
RUN 6	1.091 (1.070)	0.092 (0.093)	727 (627)
RUN 7	1.076 (1.026)	0.095 (0.089)	733 (622)
AECL Lookup Table	1.012	0.088	736

Values in parentheses are for the original model.
This number indicates the number of the predictable cases among 736 experimental data points.

Fig. 1. Schematic diagram of the physical model.

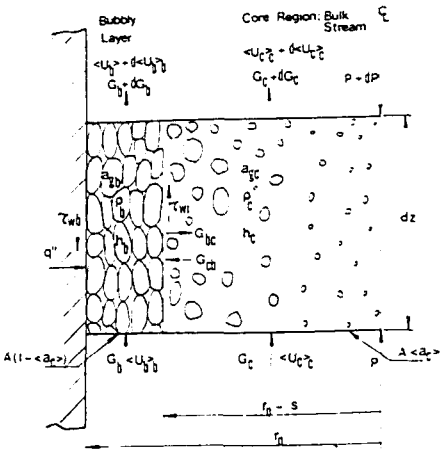

Figure 2 Comparison of predicted and measured CHF in RUN 2

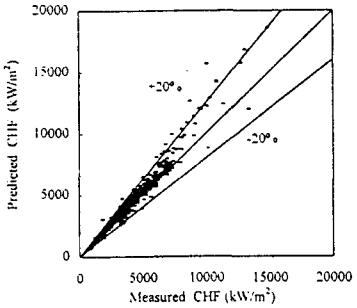

Figure 3 Dependence of prediction accuracy on pressure in RUN 2

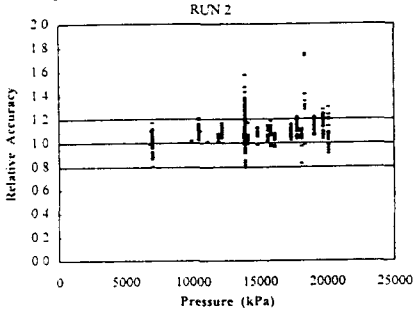

Figure 4 Dependence of prediction accuracy on mass flux in RUN 2

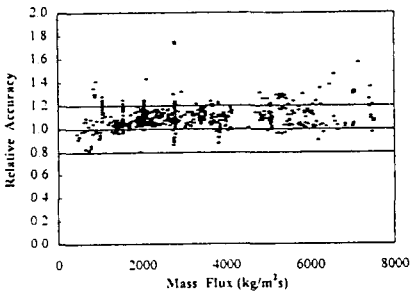

Figure 5 Dependence of prediction accuracy on exit quality in RUN 2

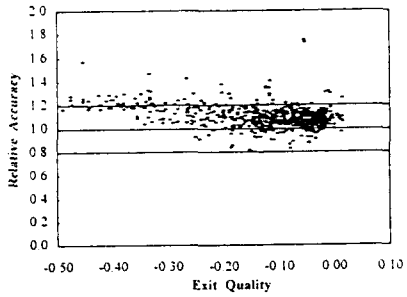

Figure 6 Dependence of prediction accuracy on L/d in RUN2